	Experiment title: "Structural assessment of unvconventional lead niobium germanate glasses with large Nb contents by High-resolution XANES & X-ray emission spectroscopy."	**Experiment number**: HE-3822
Beamline: ID26	**Date of experiment**: from: 30-5-2012 to: 3-6-2012	**Date of report**: February 2013 *Received at ESRF:*
Shifts: 9	**Local contact(s)**: Mauro Rovezzi	

Names and affiliations of applicants (* indicates experimentalists):

Roberta Morea*, José Gonzalo*, Jan Siegel*, Javier Solís*
Instituto de Optica, CSIC.
Serrano 121, E-28006 Madrid. SPAIN.

Wojciech Gawelda
European XFEL GmbH
Albert-Einstein-Ring 19, D-22761 Hamburg, GERMANY.

Report:

The aim of the experiment was to investigate the local arrangement of Nb and Ge atoms in niobium-lead-germanate thin film glasses produced by Pulsed Laser Deposition having large Nb contents (up to 55 % mol). These thin film glasses present a large nonlinear third order optical susceptibility ($/\chi^{(3)}/\approx 2\times10^{-11}$ esu at 800 nm, which is 10^3 times higher than that of SiO_2) that has been attributed to the formation of a 3-dimensional (3D) Nb-based glass structure along with the presence of a significant fraction of Nb^{4+} ions in the film glasses. For that purpose we have performed High-energy-resolution fluorescence detected (HERFD) XAS on the ID26 beamline. There were no major disruptions during the experiments and most of the planned program could be developed. All the experiments described below were performed in total fluorescence yield mode and at room temperature. Table I summarizes the composition of the studied glasses. Further details can be found in the application form.

Analysis of Ge local structure:

We have performed XANES and EXAFS experiments at the Ge K-edge. We have analyzed pellets of a GeO_2 reference (tetrahedral) and of the bulk samples (G10B and G40B), which correspond to the lowest and highest Nb content, and the corresponding thin film glasses G10F & G40F. We made 5 acquisitions in the case of XANES and 50 in the case of EXAFS in order to have a good signal to noise ratio.

Figure 1 shows the XANES spectra of the GeO_2 reference, G40B and G40F glasses (G10B and G10F spectra are similar to that of G40B and thus they are not shown here). The absorption edge, determined as the maximum of the first derivative of the absorption spectra, was found to be at $E_0\approx11110.5 \pm 0.2$ eV for all samples, which is 0.9 eV above the value measured for the reference. The inset in Fig. 1 zooms into the spectral region between 7-30 eV above the absorption edge. As it can be seen in this inset, the reference shows three resonances at 9.1, 12.5 and 21.2 eV above the edge, which are typical of 4-coordinated Ge in crystalline environment. XANES spectra of the glasses show a much more intense white line emission, whereas these resonances are less evident. We observe two resonances at 10.8 ± 0.6 and 24.1 ± 0.4 eV for

G10B, G40B, G10F, corresponding to tetrahedral vitreous GeO_2, whereas they appear at 15.0 and 26.5 eV for G40F, which is much closer to what it is expected for 6-coordinated Ge.

Figures 2a and 2b show the k^2-weighted EXAFS spectra of the analyzed samples and the corresponding Fourier transforms, respectively. Two main peaks at 1.4 and 2.8 Å are observed in the Fourier transform of the reference sample. These peaks correspond to the first neighbouring Ge-O and Ge-Ge coordination shells. The first peak is observed at a similar interatomic distance for all studied glasses. However, the second peak appears only in the case of G40B, and is hardly observable for G10B and the film glasses (G10F and G40F). This is due to the partial crystallization of G40B, which implies a much higher degree of order around Ge atoms in that sample.

Our results are consistent with the expected tetrahedral environement for Ge atoms, although the presence of a small fraction of Ge in octahedral coordination could also be possible. We present first results of the data analysis and fitting in Table 2. Here we have assumed a tetrahedral coordination for Ge and a Ge-O interatomic distance in the range 1.75-1.78 Å. The longest Ge-O distance correspond to the G40F film glass. We have included in Fig. 2b the fit results for the G40F EXAFS spectrum

Film sample	Bulk sample	$XNb_2O_5 \cdot YPbO \cdot ZGeO_2$ (mol %)
G10F	G10B	15 - 25 - 60
G1F	G1B	25- 25 - 50
G7F	G7B	35 - 35 - 30
G40F	G40B	55 - 35 - 10

Table 1. Composition of the film and corresponding bulk samples.

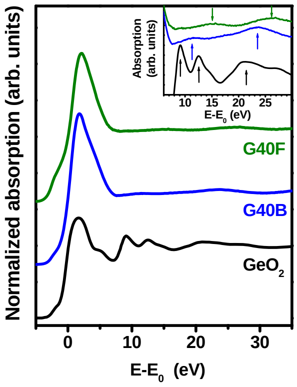

Figure 1. Normalized XANES spectra at the Ge K-edge measured for GeO_2, G40B and G40F. The inset shows an enlarged image of the post-edge region. The arrows indicate the resonances described in the text.

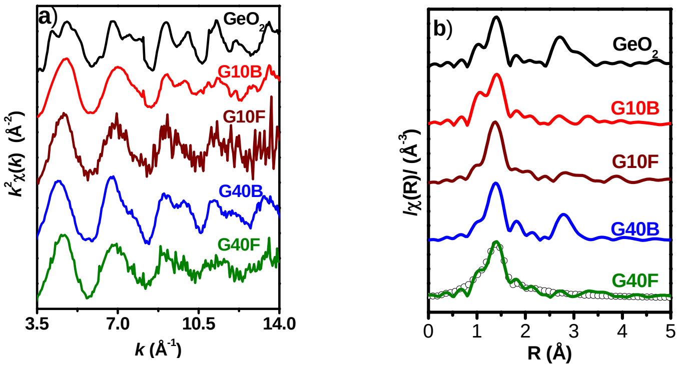

Figure 2. (a) k^2-weighted EXAFS spectra at the Ge K-edge, and (b) Modulus of the Fourier transform of the EXAFS spectra shown in (a) for GeO_2 and the analyzed glasses. The circles in G40F correspond to the fit from the data included in Table 2.

	Coord. Nº (fixed)	R(Ge-O1) R_{eff}= 1.736 Å (± 0.01 Å)	R(Ge-O2) R_{eff}= 1.740 Å (± 0.01 Å)	σ^2(Ge-O) (± 0.0005)
GeO_2	2(O1)+2(O2)	1.752	1.756	-0.0005
G10B	2(O1)+2(O2)	1.762	1.766	0.002
G10F	2(O1)+2(O2)	1.764	1.768	0.0035
G40B	2(O1)+2(O2)	1.758	1.763	0.002
G40F	2(O1)+2(O2)	1.776	1.78	0.0041

Table 2. Fit results for GeO_2 reference and Nb_2O_5-PbO-GeO_2 glasses. Phase and amplitude from tetrahedral GeO_2. Coordination number was fixed to 4.

Analysis of Nb oxidation state and local structure:

In this case we have performed both XANES and EXAFS experiments at the Nb K-edge. The number of acquisitions was between 4 and 20 for XANES, while we only could perform 1 or 2 acquisitions for EXAFS due to shortage of time. One of the specific goals of the experiments was to determine the oxidation state of Nb atoms in the glasses. Thus, we have considered three references where Nb is present in different oxidation states: metallic Nb, NbO_2 and Nb_2O_5. We have analyzed a Nb foil (only XANES), pellets of NbO_2, Nb_2O_5 and of the bulk glasses (G10B, G1B, G7B & G40B) and the thin film glasses (G10F, G1F, G7F & G40F).

Figure 3 shows the XANES spectra of the references, which constitute the basis for the analysis of the bulk and film glass spectra. The excellent energy resolution of the beam line ID26 allows us to clearly distinguish the Nb white line emission at 18988.5 eV and at 19008.2 eV in the case of metallic Nb and Nb_2O_5 respectively, whereas it appears as a shoulder in the case of NbO_2. The absorption edge values measured for the references are included in Table 3. E_0 shifts to a higher value when the oxidation state of Nb increases, this energy shift being $\Delta E \approx 1.63$ eV in Nb_2O_5 with respect to NbO_2. In addition, we clearly observe the pre-edge peak for NbO_2 and Nb_2O_5. Since Nb has an octahedral coordination in both cases, the fact that the pre-edge peak is much more intense in the case of Nb_2O_5 is related to a higher distortion of the octahedra or to the larger density of empty *d*-states of Nb^{5+} in Nb_2O_5 with respect to Nb^{4+} in NbO_2. Finally, we also observe two bands (I, II in Fig. 3) near the edge in the spectra of the oxide references. They are related to low-energy scattering resonances of photoelectrons by nearest neighbors, and are correlated to the average Nb-O distance (I) and to the degree of order around Nb atoms (II).

We have also compared the XANES spectra of samples G10B and G40B with the reference oxides (Fig. 3). XANES spectra of the other bulk samples, not shown in the figure, are similar to that of G10B. We observe in both cases an intense pre-edge peak and an absorption edge similar to that of Nb_2O_5 (Fig. 3 inset). In G40B spectrum, bands I and II are observed as well as the white line emission. However, in G10B, we only observe clearly band I, whereas band II seems to be convoluted with the white line emission band. These results indicate a more ordered environment around Nb in G40B, which is in agreement with Ge XAS analysis for this sample. Finally, we have also compared these results with those obtained for film glasses. Their XANES spectra are very close to that of G10B. Thus, only G10F and G40F spectra are shown in Fig. 3. We observe a well defined pre-edge peak and an absorption edge similar to that of the bulk samples and Nb_2O_5. Moreover, band I is positioned at the same energy and presents the same intensity for all film glasses, which suggests that the average Nb-O distance is similar for all of them. Only in G40F, bands I and II present a similar intensity. This fact has been previously related with glassy structures characterized by a 3D framework of $[NbO_6]$. Thus we can conclude that Nb is most likely in octahedral coordination with a high degree of distortion and that Nb^{4+} is not present in the glass samples.

	E_0 (eV)
Nb	18986.5
NbO_2	19004.0
Nb_2O_5	19005.6

Table 3. Edge energy values (E_0) measured for the reference samples.

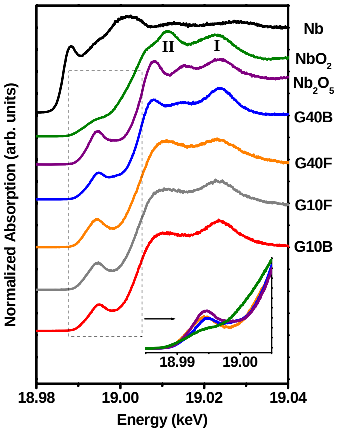

Figure 3. Normalized XANES spectra at the Nb K-edge of the reference samples and representaive bulk and film samples. The inset shows an enlarged image of the absorption-edge region. I and II refer to the edge bands described in the text.

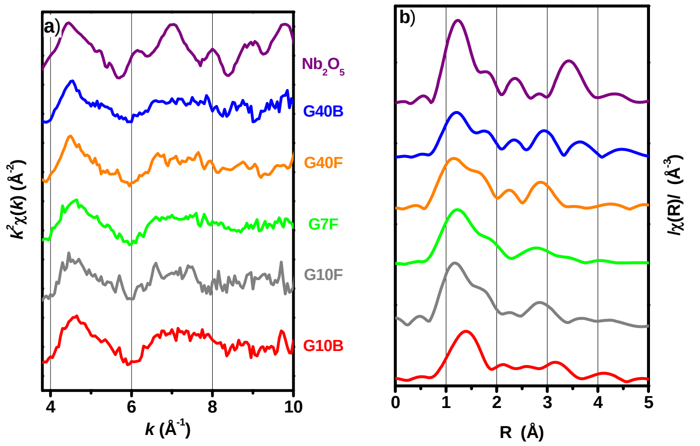

Figure 4. (a) k^2-weighted EXAFS spectra at the Nb K-edge, and (b) Modulus of the Fourier transform of the EXAFS spectra shown in (a) of Nb_2O_5 and representative bulk and film samples.

Figures 4a and 4b show, respectively, the k^2-weighted EXAFS signal and the corresponding Fourier transforms (for $k < 9$ Å^{-1}) of Nb_2O_5 and representative bulk and film glasses. We observe in Fig. 4a, a damping in the EXAFS oscillations for $k > 8$ Å^{-1}, especially in the case of film glasses (G40F and G7F). This has been related to static disorder produced by oxygen ions due to their different coordination distances and to dynamic disorder due to the measurements at room temperature. Thus, a larger number of EXAFS acquisitions at low temperature would be needed to improve the spectra. In the Fourier transform of the Nb_2O_5 reference, we observe two main bands in the range 1 to 4 Å (without shift correction). At the present time, we attribute the band peaking at 3.5 Å to first Nb neighbors, whereas the other band has been attributed in the literature to first O neighbors. In the case of bulk samples (G10B, G40B), the band at 3.5 Å disappears, while the band at 1-2 Å seems to be dependent on the Nb content in the samples. Thin film glasses G10F and G40F present features similar to their corresponding bulk glasses. Film glass G7F presents a smoother spectrum in which two bands can be distinguished in the 1-2 Å region. This may be an effect of the FT due to the damping in the EXAFS oscillations. Modeling of the Nb environment in the glasses is currently underway.

These preliminary analysis results permit us to exclude the presence of Nb^{4+} and $[NbO_4]$ groups in the film glasses, while the existence of a fraction of $[GeO_6]$ octahedra in the case of the film G40F cannot be ruled completely out at the present time. In addition, the obtained results confirm that the G40F film glass having the largest Nb content possesses a glass structure that is different from that of the other glasses and is likely formed by a 3D association of Nb octahedra. Based on that, we conclude that the nonlinear optical response observed in the case of G40F is related to structural changes rather than to the presence of extra delocalized electrons associated to Nb^{4+}.